A topological optimization procedure applied to multiple region problems with embedded sources

CTM Anflor, EL Albuquerque and LC Wrobel

CTM Anflor (corresponding author)
School of Engineering and Design
Brunel University
Uxbridge UB8 3PH
Middlesex, UK
Tel: +44 (0)7448 125116
Fax: +44 (0)1895 266882
e-mail: anflor@unb.br

EL Albuquerque
Universidade de Brasília, Faculdade de Tecnologia
Departamento de Engenharia Mecânica
Campus Universitário Darcy Ribeiro
70.910-900 - Brasília, DF - Brasil
Tel: +55 (61) 31071157
Fax: +55 (61) 31075707
e-mail: eder@unb.br

LC Wrobel
School of Engineering and Design
Brunel University
Uxbridge UB8 3PH
Middlesex, UK
Tel: +44 (0)1895 266696
Fax: +44 (0)1895 256392
e-mail: luiz.wrobel@brunel.ac.uk

Abstract The main objective of this work is the application of the topological optimization procedure to heat transfer problems considering multiple materials. The topological derivative (D_T) is employed for evaluating the domain sensitivity when perturbed by inserting a small inclusion. Electronic components such as printed circuit boards (PCBs) are an important area for the application of topological optimization. Generally, geometrical optimization involving heat transfer in PCBs considers only isotropic behaviour and/or a single material. Multiple domains with anisotropic characteristics take an important role on many industrial products, for instance when considering PCBs which are often connected to other components of different materials. In this sense, a methodology for solving topological optimization problems considering anisotropy and multiple regions with embedded heat sources is developed in this paper. A direct boundary element method (BEM) is employed for solving the proposed numerical problem.

Keywords Topological optimization, BEM, Multiple materials, Inclusions, Anisotropy

1 Introduction

Shape and topology optimization are of high importance for engineering problems. The search for optimization methods with low computational cost, which deliver the best solutions for the problem under consideration, play an important role in the academic community. The choice of the numerical method to be employed is based on a number of features. Among the numerical methods that can be classified as classical, and which have been succesfully employed for topology optimization, are the SIMP (solid isotropic method with penalization), ESO (evolutionary structural optimization) and level set methods. All these methods are generally performed by taking the finite element method (FEM) as the numerical method of choice, and are often applied for solving elasticity problems. According to Shiah et al. [1], materials with anisotropic properties have been employed for a great number of applications since the earlier 1960s. High performance is achieved when a composite is constructed by combining two or more materials. Despite its importance, very few works are found in the literature considering topology optimization for anisotropic materials aplied for heat transfer, when compared to elasticity problems. Li et al. [2] developed a computational procedure based on FEM and ESO for the topology design of heat conduction in isotropic fields. Zhang and Liu [3] developed a new method based on topology optimization for solving heat conduction problems for isotropic media with distributed heat sources. This method was able to reconstruct the conducting paths by distributing high conductive materials. Heat flow control within a composite material was studied by [4]. A gradient based optimization routine coupled with an FEM solver was employed in an iterative process for determining the distribution of the thermo-physical parameters. Based on these parameters, the optimal conductivity heat transfer path in the composite was designed. Another concept recently employed for topology optimization using BEM instead of FEM is the topological derivative [5,6]. Some results employing D_T were also performed using FEM, but it is worth noting that the BEM characteristics are attractive for optimization procedures once this method has no mesh dependence and low computational cost. The D_T measures the sensitivity of a given shape functional when the domain is perturbed by an infinitesimal perturbation, such as the insertion of holes, inclusions and even cracks. This concept has been successfully used for a wide range of problems in addition to topology optimization, such as image processing [7] and fracture mechanics [8]. Many efforts for extending this concept for more complex problems have been done in the last years. Recently, [9,10] obtained a closed form for the D_T considering the total potential energy associated to an anisotropic and heterogeneous heat difusion problem, when a small circular inclusion of the same nature of the bulk phase is introduced at an arbitrary point of the domain. This closed formula was derived in its general form and particularized for heterogeneous and isotropic media, showing agreement with the Amstutz [11] derivation. On the basis of previous relevant work by one of the authors [5,12], this paper aims at extending an optimization procedure for heat transfer problems considering heterogeneous materials using BEM and D_T. The derivation of an integral equation valid over all the external boundaries of the different material regions, without due consideration for the interfaces between them, is not impossible, despite the complexity involved. Alternatively, a conforming mapping technique is implemented to reduce the steady-state anisotropic field to an equivalent isotropic domain, avoiding some new derivations [1]. The influence of the anisotropic conductivity properties imposed to the inclusion and matrix on the final topology will be investigated. The manuscript is organized as follows. The BEM

treatment of multi-domain mapping is described in Section 2. In Section 3, the architecture of the optimization process is presented, as well as the D_T sensitivity formula used. A sample of two-dimensional numerical problems is outlined. The numerical results are presented and discussed in Section 5. Finally, the conclusions are given in Section 6.

2 BEM treatment of multi-domain mapping

Many research works have devoted substantial efforts on developing efficient and robust topology optimization procedures during the last decades. The present work is focused on anisotropic multi-regions for heat diffusion problems. When dealing with non-homogeneous composites, it is usually necessary to split the domain into several different materials held together, and treat each one in turn. The derivation of an integral equation valid over all the external boundaries of the different material regions without due consideration for the interfaces between them is not impossible, despite the complexity involved. Alternatively, a conforming mapping technique can be used to reduce the steady-state anisotropic field to an isotropic equivalent domain, avoiding some new derivations. Some works have successfully employed a linear coordinate transformation for solving anisotropic thermal field problems with FEM and/or BEM. The first works devoted to the mapping technique were presented by [13,14]. Recently, Shiah and Tan [15] presented a method for reducing a three-dimensional steady-state anisotropic field problem to an equivalent isotropic one, governed by the Laplace equation in a mapped domain. Another work presented by [1] expanded this technique to the heat conduction in composites consisting of multiple anisotropic media for 2D and 3D. Despite the mapping technique formulation being available for 3D problems, only 2D problems have been considered. Furthermore, the D_T formula for calculating the domain sensitivities due to a perturbation caused by the insertion of a small inclusion is only valid for 2D problems [9]. Problems governed by the Poison equation are well known in the BEM literature [16]. The boundary integral equation for this problem is as follows:

$$\begin{aligned} c(\eta)\,\phi(\eta) &= \int_{\Gamma} q(\eta,\xi)\,U(\eta,\xi)\,d\,\bar{\Gamma}(\xi)... \\ &-\int_{\Gamma} \phi(\xi)\,U(\eta,\xi)\,d\,\bar{\Gamma}(\xi) - \sum_{m=1}^{n} \overline{b_m}\,U(\eta,M_n) \end{aligned} \tag{1}$$

where ϕ and q represent the temperature and its normal gradient, respectively. The variable n represents the unit outward normal vector along the boundary while $\bar{\Gamma}$ is used to denote the boundary on the mapped domain.

The source and field points are designated by the variables η and ξ. The value of $c(\eta)$ depends on the geometry at η. The variable $\overline{b_m}$ is the mth internal heat-source point. The fundamental solutions for the potential and its gradient are represented by $U(\eta,\xi)$ and $T(\eta,\xi)$ and given by,

$$\begin{aligned} &U(\eta,\xi) = \frac{1}{4\pi r} \quad \text{and} \quad T(\eta,\xi) = -\frac{1}{4\pi r^2} n_i r_{,i} \quad \textit{for} \quad 3D \\ &U(\xi) = \frac{1}{2\pi}\,\ln\left(\frac{1}{r}\right) \quad \text{and} \quad T(\xi) = -\frac{1}{2\pi r} n_i r_{,i} \quad \textit{for} \quad 2D \end{aligned} \tag{2}$$

After the usual discretization of the boundary into boundary elements, eq. (1) is applied at each boundary nodal point (η), generating the system of equations for a single domain. The original geometry (Γ) is mapped into an isotropic equivalent domain $(\overline{\Gamma})$ by using a linear coordinate transformation,

$$\left[X_1 \;\; X_2\right] = \left[F(K_{ij})\right]\left[x_1 \;\; x_2\right]^T$$
$$\left[x_1 \;\; x_2\right] = \left[F^{-1}(K_{ij})\right]\left[X_1 \;\; X_2\right]^T$$

where K_{ij} is the conductivity coefficient and $\left[F(K_{ij})\right]$ as well as $\left[F^{-1}(K_{ij})\right]$ are defined by,

$$F = \begin{bmatrix} \sqrt{\Delta}/K_{11} & 0 \\ -K_{12}/K_{11} & 1 \end{bmatrix}; \qquad F^{-1} = \begin{bmatrix} K_{11}/\sqrt{\Delta} & 0 \\ -K_{12}/\sqrt{\Delta} & 1 \end{bmatrix}; \qquad \Delta = K_{11}K_{22} - K_{12}^2$$

Now, the collocation process for solving the integral equation (1) should be done on the distorted domain and this procedure also requires a mapping of the Neumann boundary conditions, as depicted in Figure 1. It is important to note that the nodal potentials remain unchanged for corresponding points between the physical (x_1, x_2) and mapped coordinate systems (X_1, X_2), since the temperature is a scalar field.

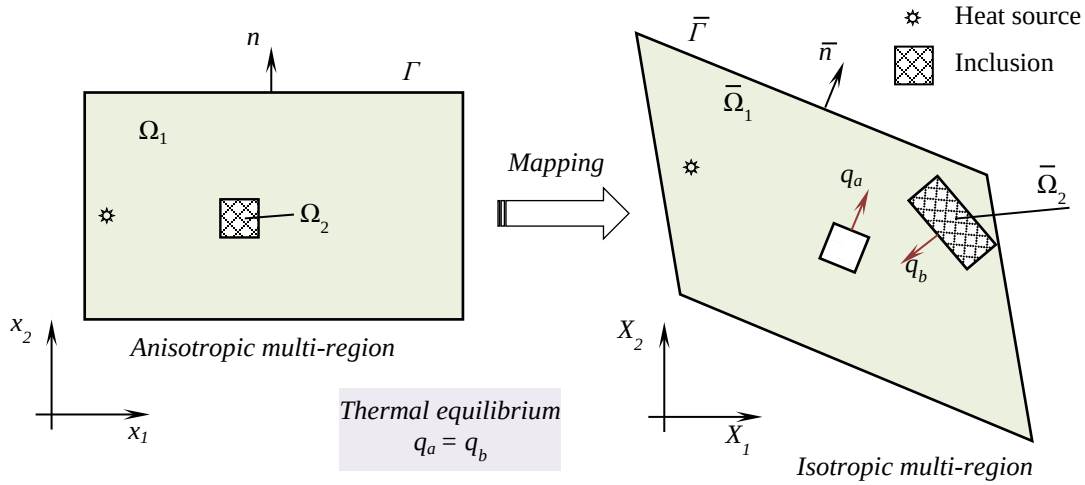

Fig. 1 Direct domain mapping of a composite material

The Neumann boundary conditions are mapped according to the relation,

$$\frac{dT}{d\bar{n}} = \left(\frac{\partial T}{\partial x_1}\frac{K_{xx}}{\sqrt{\Delta}} + \frac{\partial T}{\partial x_2}\frac{K_{xy}}{\sqrt{\Delta}}\right)\bar{n}_1 + \left(\frac{\partial T}{\partial x_2}\right)\bar{n}_2 \tag{3}$$

Taking into account the boundary conditions imposed to the problem, a set of simultaneous equations for unknown and known temperature or its normal derivative at nodal points may now be solved by standard methods. Once the system of equations is solved, an inverse mapping must be further employed for recovering the potential gradients on the original domain, as follows,

$$\frac{dT}{dn} = \overline{\varphi}_i^T F \frac{F^T \overline{n}^T}{\left| F^T \overline{n} \right|} \tag{4}$$

where $\overline{n}$ is the outward normal vector on the mapped domain. The variables $\overline{\varphi_i}$ represent the temperature gradients along the mapped boundary, and are defined as,

$$\overline{\varphi}_i^T = \left(\frac{\partial T}{\partial X_1} \quad \frac{\partial T}{\partial X_2} \right) \tag{5}$$

with each temperature gradient of eq.(5) calculated by

$$\begin{aligned} \partial T / \partial x_1 &= \left(dT / d\overline{n} \right) \overline{n}_1 \\ \partial T / \partial x_2 &= \left(dT / d\overline{n} \right) \overline{n}_2 \end{aligned} \tag{6}$$

When dealing with non-homogeneous media, appropriate thermal compatibility and equilibrium conditions along the interfaces of conjoint materials must be supplied. As explained before, when the anisotropic domain is transformed to an equivalent isotropic one, it results in a deformed geometry. The inserting of an inclusion with different properties inside the matrix will result in an overlap or separation of the interfaces of the conjoint materials (see Figure 1). For a non-cracked interface between isotropic materials, the compatibility equation is imposed as

$$T^1 = T^2 \tag{7}$$

where the superscripts denote materials 1 and 2, respectively. The above relation still holds for anisotropic materials, but special conditions are required for the temperature gradient due to the misalignment of the mapped interfaces. As a consequence of their distortion, the thermal equilibrium of the normal heat fluxes must be reformulated accordingly. The sum of the normal fluxes across the interfaces must vanish in order to satisfy the thermal equilibrium between adjacent materials, as follows (see Shiah et al. [1]),

$$\sum_{m=1}^{2} K_{ij}^{(m)} T_{,j}^{(m)} n_i^m = 0 \tag{8}$$

The unit outward normal vectors along the boundary surface of the coordinate systems are related by,

$$\begin{aligned} n_1 &= \frac{\left(n_1 \sqrt{\Delta} / K_{11} - n_2 \ K_{12} / K_{11} \right)}{\Omega} \\ n_2 &= n_2 / \Omega \end{aligned} \tag{9}$$

where Ω is defined as,

$$\Omega = \sqrt{\left(\overline{n_1} \sqrt{\Delta} / K_{11} - \overline{n_2} \, K_{12} / K_{11} \right)^2 + \overline{n_2}} \tag{10}$$

Substituting eq.(9) into eq.(8) and carrying out some algebraic processes leads to a general thermal equilibrium form which takes into account the balance of the normal heat fluxes across the two adjacent anisotropic materials,

$$\sum_{m=1}^{2} \frac{\Delta^{(m)}}{\Omega^{(m)} K_{11}^{(m)}} \cdot \frac{dT^{(m)}}{dn^{(m)}} = 0 \tag{11}$$

It is worth noting that only a 2D formulation was presented here, as the topology optimization is only performed for two-dimensional problems. Furthermore, to the authors' knowledge, there is no D_T available for evaluating the domain sensitivity for 3D problems perturbed by the insertion of inclusions.

3 The architecture of the optimization process

This section describes how a conformal mapping for multiple materials is implemented in an existing BEM code for the mapping of a steady-state anisotropic field into an equivalent isotropic one. The code was initially written for solving topology problems considering a single material. The topology optimization process was performed creating voids inside the domain and a final geometry was generated with less volume [12]. In this paper, a different material will be added during the optimization process instead of removing material. Therefore, a multiple regions technique combined to a conformal mapping is implemented, characterizing a multiple anisotropic media problem. For the optimization process, a special subroutine was developed for detecting the overlap or even the superposition of the conjoint surfaces due to the misalignment resulting from the geometry mapping, as depicted in Figure 1. A general thermal-equilibrium equation was conveniently applied on the boundaries. The topological optimization is performed using sensitivity analysis by D_T. This procedure will produce new topologies with multiple materials in order to achieve the best thermal performance. A typical Printed Circuit Board is manufactured with multiple materials, where the main matrix is filled with different electronic components (chips). In this sense, a second material could be added which would act as an insulator, or even to design an optimal thermal path to efficiently cool the device. Considering a topology optimization problem, the steps involved for solving a multiple material problem are illustrated in Figure 2 and can be summarized as:

Step 1 *– The initial problem is formulated. A linear transformation is used if the problem presents a non-isotropic behavior, i.e., {$K_{xy} \neq 0$ and $k_{xy} \neq 0$}. The capital K and the lower case k denote the thermal properties of the matrix and the inclusions, respectively. The mapped problem is solved using the BEM solver.*

Step 2 *–The D_T is used for determining the domain sensitivity.*

Step 3 *– Those areas with lower sensitivity will have a new material inserted, which would provide insulation or a high conductivity performance.*

Step 4 *– Join the materials and impose the compatibility and thermal-equilibrium conditions presented in eq.(7) and eq.(11), respectively.*

Step 5 *– Check the stop criteria.*

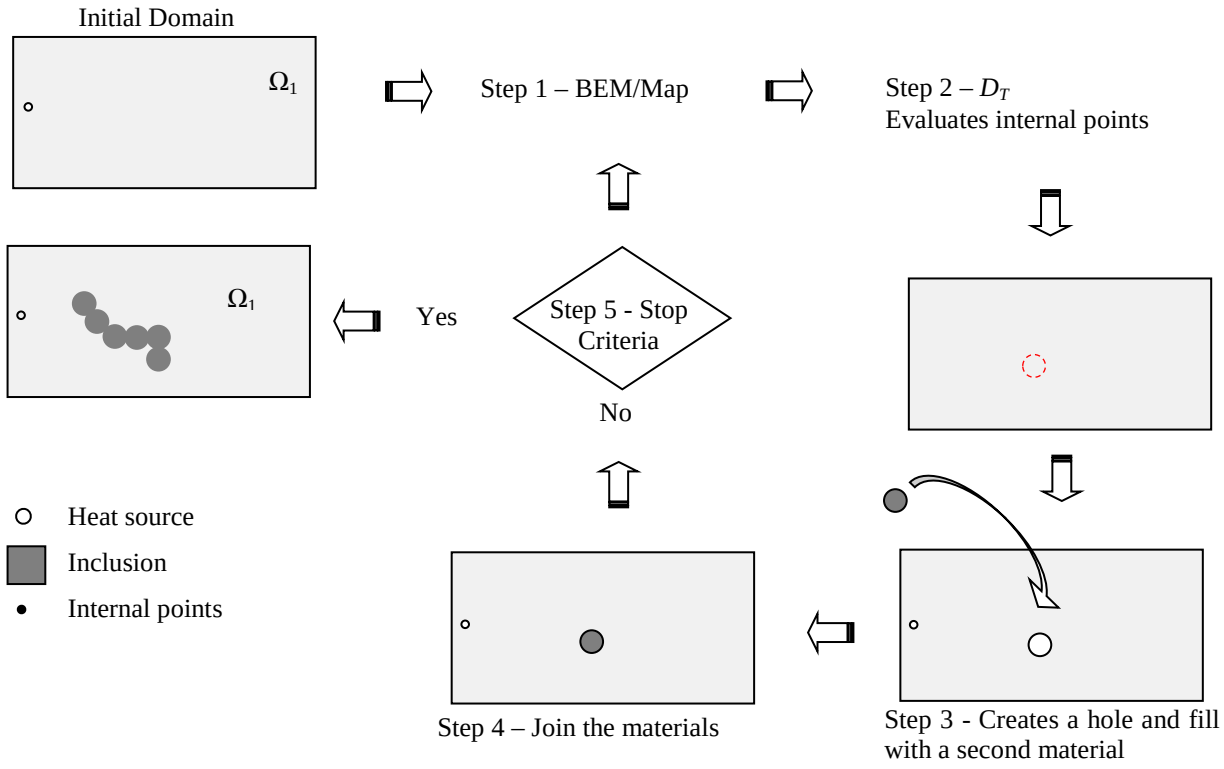

Fig. 2 Details for optimization process

A closed formula proposed by [9] for D_T is employed for determining the sensitivity of the conductivity tensor when an inclusion is introduced at an arbitrary point of the domain. The D_T is a scalar field over Ω that depends only on the conductivity tensor of the matrix and the inclusion, and on the solution of the thermal equilibrium problem for the original unperturbed domain,

$$k^*(\bar{y}) = \begin{cases} k^i = \gamma k_m & \bar{y} \in \Omega^m \end{cases} \tag{12}$$

where $\bar{y}$ denotes the centre of the circular perturbation, while γ defines the ratio between the conductivity of the matrix (k^m) and the conductivity of the perturbation (k^i). The sensitivity of the macroscopic conductivity tensor to the topological change due to the insertion of a small inclusion is presented in closed form as

$$D_T(\bar{y}) = 2k^m \frac{k^m - k^i}{k^m + k^i} \left|\nabla u(\bar{y})\right|^2 \qquad \forall \bar{y} \in \Omega \tag{13}$$

It is important to note that D_T is a scalar field over Ω that depends only the conductivity parameters and on the solution of the thermal equilibrium problem for the original domain (Ω).

4 Numerical Results

Some tests are now presented in order to assess the proposed algorithm. All examples are discretized with constant boundary elements. All conduction fields to be designed consist of two materials, one with thermal conductivity $\{K_{xx}, K_{yy}, K_{xy}\}$ and another insulating material with conductivity $\{k_{xx}, k_{yy}, k_{xy}\}$. The first case refers to a standard benchmark test used for PCB substrates, with the final topology compared with previous results presented by Liu et al. [17]. The second example presents a cross heat conductor where the influence of isotropy, orthotropy and anisotropy conditions on the topology is studied. The third example represents a three heat sources conductor where a fully isotropic optimization and another case taking into account the conversion from anisotropy to isotropy behaviour are studied. From the second case on, the percentage amount of inclusions will be calculated as $((1-V/V_o)\cdot 100)$, where V is the volume at an specific iteration and V_o is the initial volume for all cases. This provides a simplified criterion to compare the topologies generated for isotropic, orthotropic and anisotropic media, starting from the same design.

4.1 Printed circuit board

A previous benchmark test investigated by Liu et al. [17] is revisited here. The problem refers to a PCB substrate with four heat sources inside the domain with a constraint zone, as depicted in Figure 3. This PCB is a rectangular plate with dimensions 33 x 53 mm, and the intensity of the heat sources is set as 100 W/m^2. The heat sources simulate the heat generated by major electronic components mounted on the PCB. The BEM model used for this case employed an initial mesh of 32 constant elements. All external edges have prescribed temperature of 0°C. The process was halted when a target of 30% of inserting material was achieved. Figure 4 depicts the topology history. It is worth to note the insertion of insulating material near the corners of the PCB.

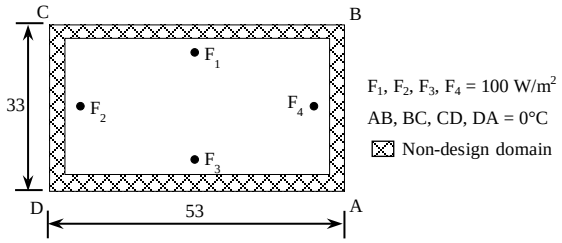

Fig. 3 PCB initial design and boundary conditions

Despite the present approach using insulating inclusions instead of voids, good agreement is obtained (see Figure 5) with the previous results of [17] and [12].

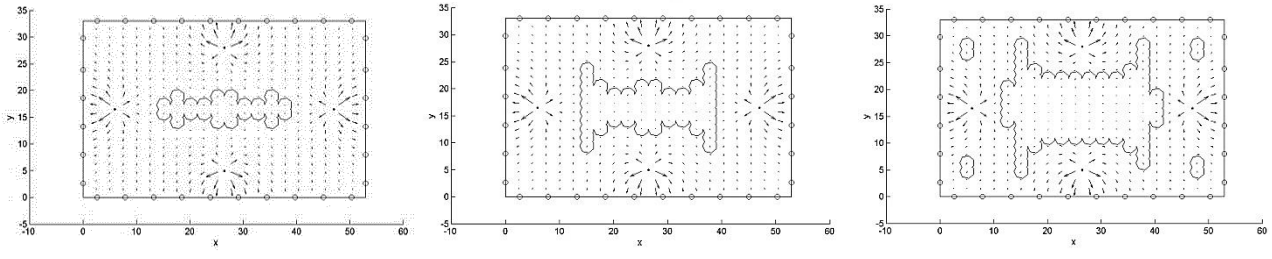

Iteration #4 Iteration #7 Iteration #23

Fig. 4 Topology evolution for the PCB

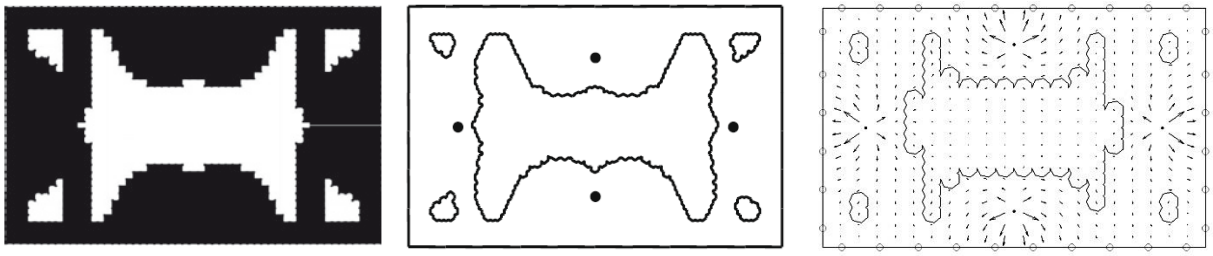

(a) (b) (c)

Fig. 5 Comparison of final topologies obtained for the PCB: a) Liu et al. (1999), b) Anflor and Marczak (2009), and c) Present results

4.2. Cross Heat Conductor

In this example the effect of isotropic, orthotropic and anisotropic characteristics in the final topologies will be investigated. The conductor is to be optimized until a target close to 27% of material inclusion is achieved. For this case, a square domain of 30 x 30 mm is subjected to high and low temperatures prescribed at its corners as depicted in Figure 6. The inclusion shape is set as a circle discretized with 6 constant elements.

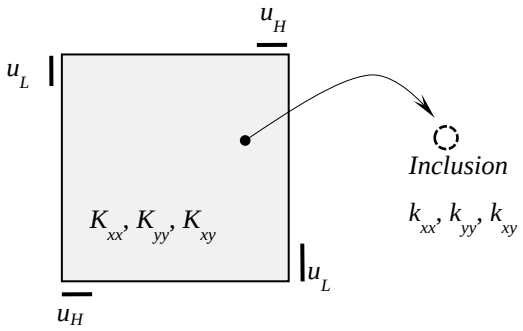

Fig. 6 Boundary conditions and thermal properties

4.2.1. **Isotropic matrix and inclusions**. The first case under consideration is totally isotropic. The thermal conductivity tensor is set as $\{K_{xx}=100,\ K_{yy}=100,\ K_{xy}=0\}$ for the matrix and $\{k_{xx}=1,\ k_{yy}=1,\ k_{xy}=0\}$ for the inclusion. During the optimization procedure, an insulating isotropic material will be progressivelly inserted into the matrix. Figure 7 illustrates the topology evolution until a 26.63% amount of insulated material is inserted.

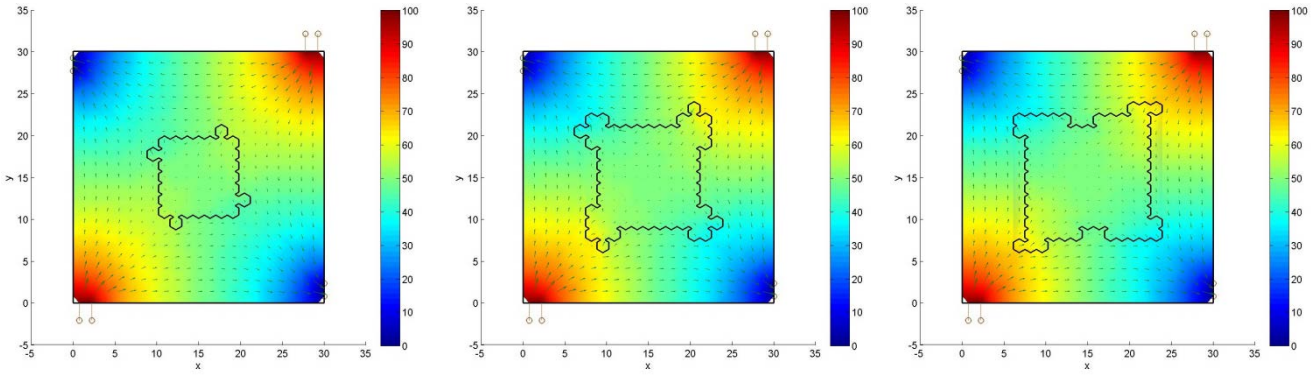

Iteration #8 - Inclusions = 11.51% Iteration #13 - Inclusions = 21.64% Iteration #16 - Inclusions = 26.63%

Fig. 7 Topology evolution for isotropic cross heat conductor: $\{K_{xx}=100,\ K_{yy}=100,\ K_{xy}=0,\ k_{xx}=1,\ k_{yy}=1,\ k_{xy}=0\}$.

4.2.2 **Orthotropic matrix and isotropic inclusions**. This case is similar to the previous one except for the orthotropic thermal conductivity tensor imposed to the matrix as $\{K_{xx}=100, K_{yy}=25, K_{xy}=0\}$. The inclusions were set as isotropic, i.e., $\{k_{xx}=1, k_{yy}=1, k_{xy}=0\}$. Figure 8 depicts the topology evolution until 27.53% of inclusions are inserted inside the matrix. As the main direction of heat transfer is the *x* direction, the final topology results in a rectangular shape. As expected, the heat flux along the *x* direction is increased.

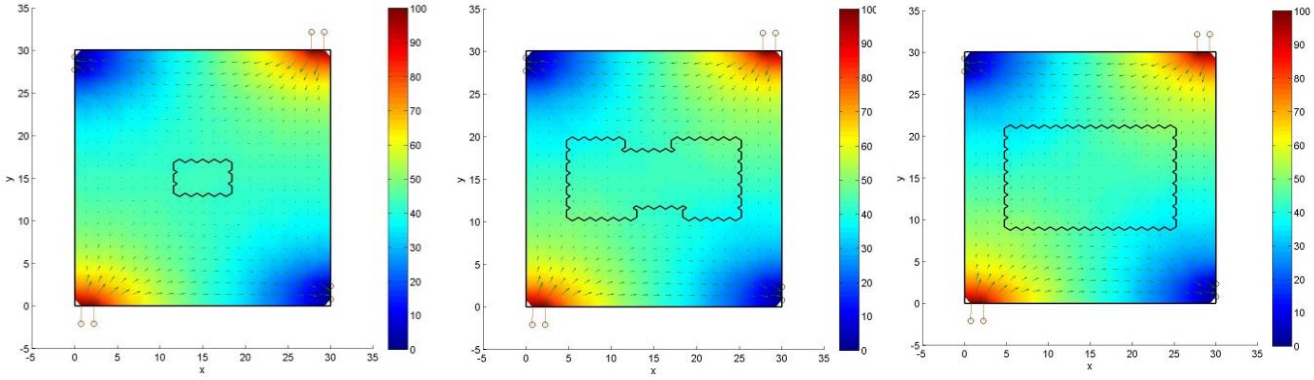

Iteration #7 - Inclusions = 7% Iteration #11 - Inclusions = 21.36% Iteration #17 - Inclusions = 27.53%

Fig. 8 Topology evolution for orthotropic cross heat conductor: $\{K_{xx}=100, K_{yy}=25, K_{xy}=0, k_{xx}=1, k_{yy}=1, k_{xy}=0\}$

4.2.3. **Isotropic matrix and anisotropic inclusions**. For this third case, the thermal conductivity tensor for the matrix is defined as $\{K_{xx}=100, K_{yy}=100, K_{xy}=0\}$ while for the inclusions it is set as $\{k_{xx}=1, k_{yy}=1, k_{xy}=0.5\}$. The main goal focuses on investigating the influence on the topology when inclusions with anisotropic characteristics are inserted inside an isotropic domain. As the iterative process evolves, it is possible to verify that the internal shape formed by inserting inclusions presents a rhombic geometry, see Figure 9. This is explained by the main axis of the cavities not being parallel to the main axis of the constitutive material.

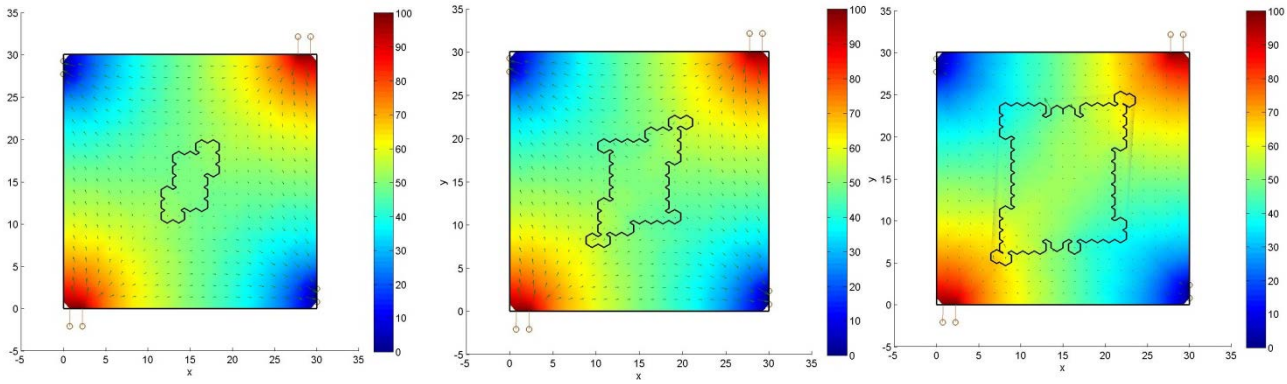

Iteration # 6 - Inclusions = 5.78% Iteration # 12 - Inclusions = 11.40% Iteration # 28 - Inclusions = 26.98%

Fig. 9 Topology evolution for cross heat conductor with anisotropic inclusions: $\{K_{xx}=100, K_{yy}=100, K_{xy}=0, k_{xx}=1, k_{yy}=1, k_{xy}=0.5\}$

Finally, a comparison between the final topologies considered in Section 4.2 is presented in Figure 10. For comparison, all cases had their iterative optimization process halted when an amount of approximately 27% of inclusions was reached. The final shapes present distinct topologies, showing the influence of the tensor thermal properties for the heat transfer process. Symmetry was not used to provide a direct comparison to the subsequent cases (which cannot use symmetry).

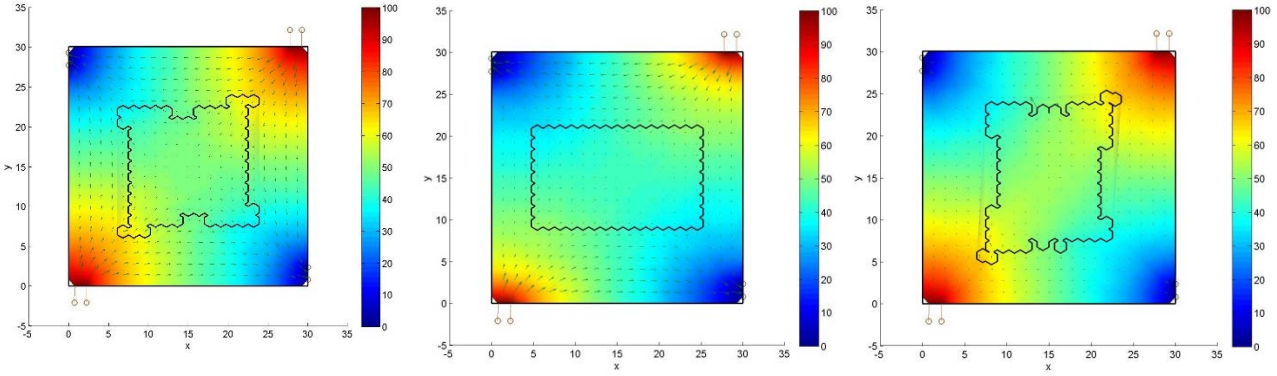

(a) Isotropic - Inclusions = 26.63% (b) Orthotropic - Inclusions = 27.53% (c) Anisotropic - Inclusions = 26.98%

Fig. 10 Final topologies for: (a) Isotropic, (b) Orthotropic and (c) Anisotropic examples

Figure 11 presents the material insertion history for the isotropic, ortotropic and anisotropic cases. For the isotropic and orthropic cases the target percentage of inclusions was almost reached at the same time, i.e., iterations 16 and 17, respectively. When dealing with the insertion of anisotropic inclusions, the optimization process took 28 iterations to reach the target percentage.

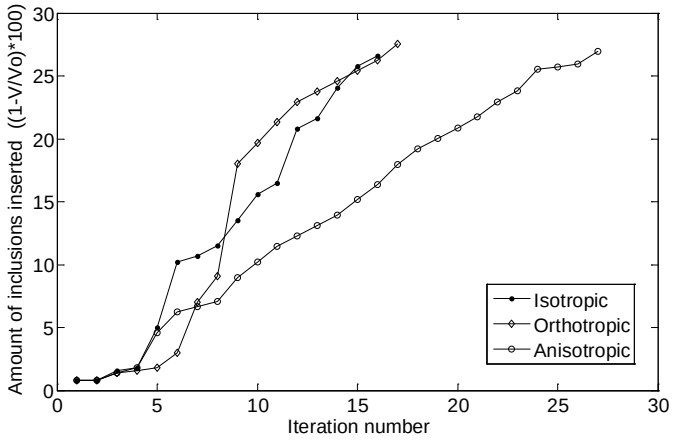

Fig. 11 Material insertion history for isotropic, orthotropic and anisotropic behaviour

4.3 Three heat sources conductor

A region of 30x30 mm is taken into account again here, but now three heat sources and a heat flux are prescribed on its boundaries, as illustrated in Figure 12. The heat source temperature and the heat flux are set as u=100°C and q=30 W/mm^2, respectively. The remaining external boundaries are all insulated.

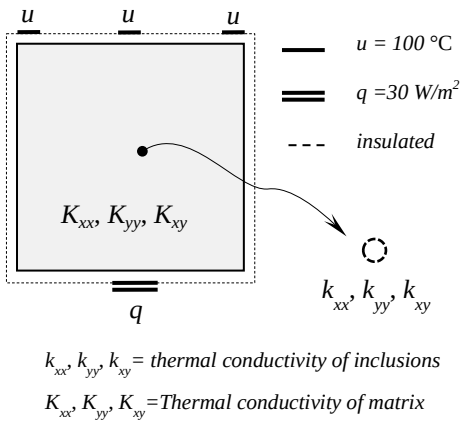

Fig. 12 Initial design for the three heat sources conductor

4.3.1 **Isotropic matrix and inclusions**. For this case the matrix thermal conductivity was set as $\{k_{xx}=100, k_{yy}=100, k_{xy}=0\}$ while for the inclusions it was set as $\{k_{xx}=1, k_{yy}=1$ and $k_{xy}=0\}$. The changes of the temperature field as the percentage of inclusions is increased is shown in the colour map presented in Figure 13, which also shows the evolution history at iterations 5, 13 and 17.

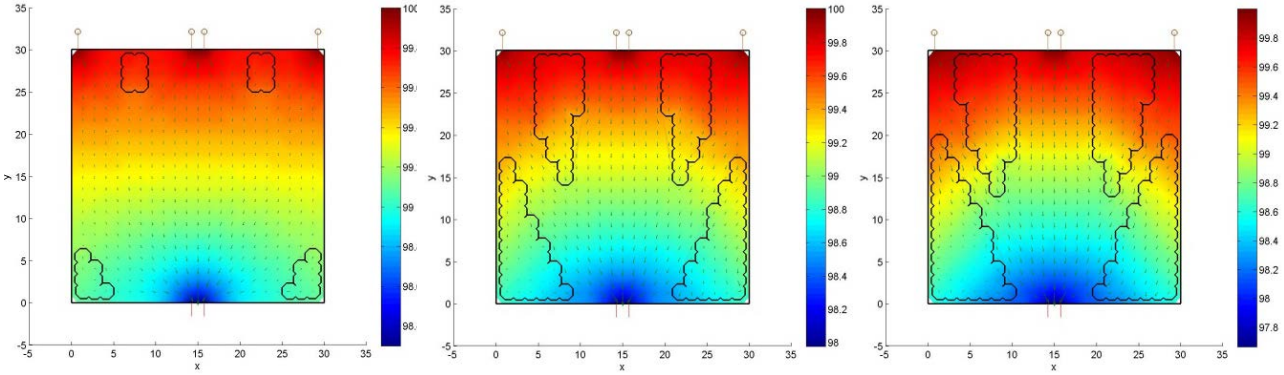

Iteration #5 - Vol = 89.83% Iteration #13 - Vol = 62.24% Iteration #17 - Vol = 53.14%

Fig 13 Evolution history for isotropic three heat sources conductor

4.3.2. **Anisotropic matrix and inclusions**. This example is employed to show the anisotropic behaviour produced by imposing the thermal properties as $\{K_{xx}=75, K_{yy}=75, K_{xy}=25, k_{xx}=1, k_{yy}=1, k_{xy}=0.5\}$. Figure 14 depicts the evolution history until the percentage of inserting inclusions reach a target close to 53%. At iteration number 57, it is possible to see that a large amount of insulating material was inserted on the right side, resulting in a delay of the heat transfer in that region.

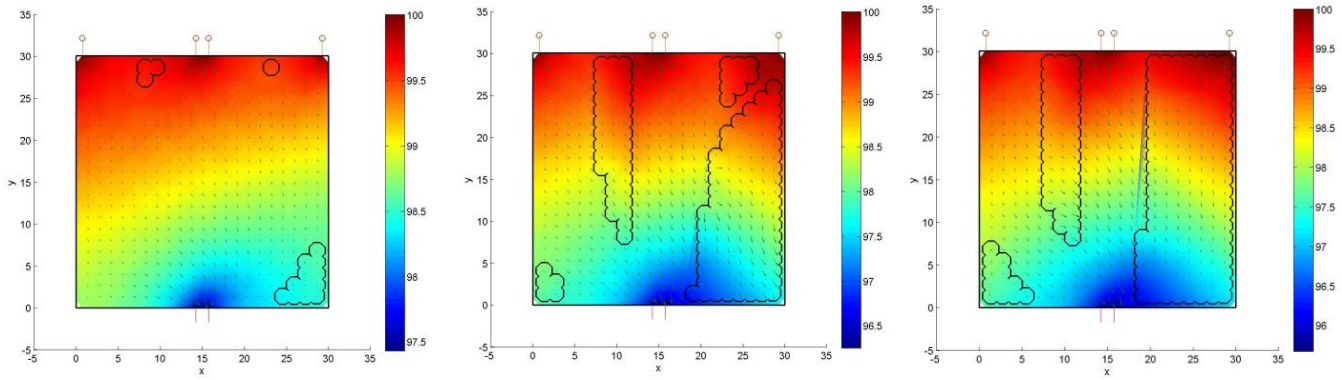

Iteration #7 - Vol = 95.06% Iteration #32 - Vol = 62% Iteration #57 - Vol = 53.15%

Fig 14 Evolution history for anisotropic three heat sources conductor

During the optimization process, a temperature control point was set at the middle bottom of the plate. The evolution history at the temperature control point, as well as the amount of inclusion inserted per iteration, are presented in Figure 15(a) and Figure 15(b), respectively. As the material insertion was more concentrated at the rigth side a temperature reduction was achieved for the anisotropic case, see Figure 15(a). Another interesting issue relies on the amount of material inserted. For the isotropic case the influence of the insertion of the inclusions was not so strong when comparing to the resulting topology with anisotropic characteristics. This observation can be verified in Figure 15(b), where the isotropic case took only 17 iterations against 57 iterations performed for the anisotropic case.

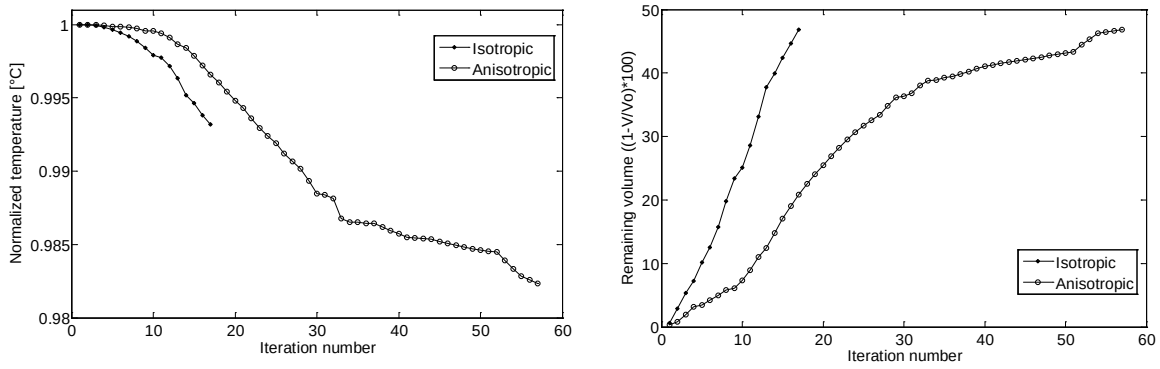

(a) (b)

Fig 15 Evolution history for three heat sources conductor: (a) Temperature and (b) Amount of inclusions inserted

4.3.3. **Anisotropic matrix and isotropic inclusions**. The main goal of this example is to show the transformation of an initially anisotropic domain into an isotropic one. In this case, an anisotropic matrix will be filled with inclusions of isotropic thermal properties. The conductive thermal tensor was set as {K_{xx}=100, K_{yy}=100 and K_{xy}=50, k_{xx}=1, k_{yy}=1, k_{xy}=0}. Figure 16 shows the optimization process history after the initial domain has been almost fully filled with 96.66% of isotropic inclusions.

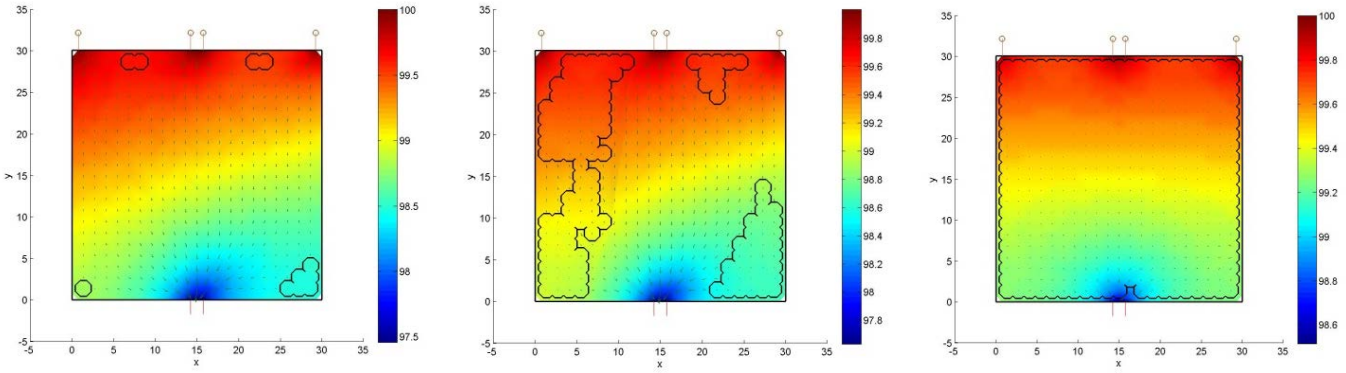

Iteration # 4 - Inclusions = 3.85% Iteration # 24 - Inclusions = 33.50% Iteration # 83 - Inclusions = 96.66%

Fig. 16 Evolution history: Anisotropic to isotropic behaviour

5 Conclusions

In this work, a topology optimization procedure was extended to multiple materials considering heat embedded sources for anisotropic problems. The derivation of an integral equation valid over all the external boundaries of the different material regions without due consideration for the interfaces between them is not impossible, despite the complexity involved. In this work, an alternative procedure involving a conforming mapping technique was implemented to reduce the steady-state anisotropic field to an equivalent isotropic domain. Furthermore, the BEM optimization procedure was successful from the point of view of computational cost, since the BEM presents no internal mesh dependency as one of its main characteristics. The proposed scheme was shown to be effective for a number of cases, and the final topologies obtained were compared with other solutions from the literature when available. The proposed methodology should be useful for designing high performance heat transfer topologies involving the coupling of different materials. Finally, the application of designed anisotropic materials for the efficient energy management of heat conduction fields will be explored.

6 Acknowledgments

Carla T.M. Anflor thanks the financial support received from CNPQ – Brazil through the Science without Borders program and from Brunel University, for developing this research.

7 References

[1] Y.C. Shiah, P. Hwang, R. Yang, Heat conduction in multiply adjoined anisotropic media with embedded point heat sources. Journal of Heat Transfer 128 (2006) 207-214.

[2] Q. Li, G.P. Steven, Y.M. Xie, O.M. Querin, Evolutionary topology optimization for temperature reduction of heat conducting fields. International Journal of Heat and Mass Transfer 47 (2004) 5071-5083.

[3] Z. Zhang, S. Liu, Design of conducting paths based on topology optimization. Heat and Mass Transfer 44 (2008) 1217-1227.

[4] E.M. Dede, Simulation and optimization of heat flow via anisotropic material thermal conductivity. Computational Science 50 (2010) 510-515.

[5] C.T.M. Anflor, R.J. Marczak, Topological optimization of anisotropic heat conducting devices using Bezier-smoothed boundary representation. Computer Modeling in Engineering & Sciences 78 (2011) 151-168.

[6] C. Bertsch, A.P. Cisilino, N. Calvo, Topology optimization of three-dimensional load-bearing structures using boundary elements. Advances in Engineering Software 41 (2010) 694-704.

[7] B.C. Patel, G.R. Sinha, K. Thakur, Early detection of breast cancer using a modified topological derivative based method. International Journal of Pure and Applied Science and Technology 7 (2011) 75-80.

[8] N.V. Goethem, A.A. Novotny, Crack nucleation sensitivity analysis. Mathematical Methods in the Applied Sciences 33 (2010) 1978-1994.

[9] S.M. Giusti, A.A Novotny, E.A. de Souza Neto, R.A. Feijóo RA, Sensitivity of the macroscopic thermal conductivity tensor to topological microstructural changes. Computer Methods in Applied Mechanical and Engineering. 198 (2009) 727-739.

[10] S.M. Giusti, A.A. Novotny, Topological derivative for an anisotropic and heterogeneous heat diffusion problem. Mechanics Research Communications, 46 (2012) 26-33.

[11] S. Amstutz S, Sensitivity analysis with respect to a local perturbation of the material property. Asymptotic Analysis 49 (2006) 87–108.

[12] C.T.M. Anflor, R.J. Marczak, A boundary element approach for topology design in diffusive problems. International Journal of Heat and Mass Transfer 52 (2009) 4604–4611.

[13] Y.C. Shiah, C.L. Tan, BEM treatment of three-dimensional anisotropic field problems by direct domain mapping. Engineering Analysis with Boundary Elements 28 (2004) 43-52.

[14] K.C. Poon, R.H.C. Tsou, Y.P. Chang, Solution of anisotropic problems of first class by coordinate-transformation. Journal of Heat Transfer 101 (1979) 340–345.

[15] K.C. Poon, Transformation of heat conduction problems in layered composites from anisotropic to orthotropic. Letters of Heat and Mass Transfer 6 (1979) 503–511.

[16] L.C. Wrobel LC, The Boundary Element Method, Wiley, Chichester, 2002.

[17] Q. Li, G. Steven, O. Querin, Y. Xie, Shape and topology design for heat conduction by evolutionary structural optimization, Int. J. Heat and Mass Transfer 42 (1999) 3361-3371.